

Minimum-fuel Powered Descent in the Presence of Random Disturbances

Jack Ridderhof* and Panagiotis Tsiotras[†]
Georgia Institute of Technology, Atlanta, GA, 30332, USA

It has recently been shown that minimum-fuel powered descent guidance can be solved onboard the spacecraft as a convex optimization problem. It therefore presents itself as a promising technology to enable future planetary exploration missions. However, since this approach is formulated as a deterministic optimal control problem, the resulting guidance law is only designed for a single pair of initial and target states without external disturbances. This paper is an attempt to extend this approach to the more general case of steering the initial position and velocity distributions to some target position and velocity distributions, while considering Brownian motion process noise acting on the system. It is shown that when using a stochastic model for powered descent, the design of the reference trajectory is coupled with the closed-loop control law through probabilistic constraints on the control.

I. Introduction

Entry, Descent, and Landing (EDL) is the process of a spacecraft entering a planet's atmosphere, decelerating from orbit, and descending to a safe landing site on the planet's surface. Atmospheric disturbances, localization error, and other factors contribute to substantial deviations from the nominal descent trajectory, which must be accounted for when selecting a landing target. This work focuses on the Powered Descent (PD) phase, during which the spacecraft uses chemical rocket engines to simultaneously steer and decelerate to a target touchdown point.

In recent works,^{1,2} Powered Descent Guidance (PDG) has been posed as a convex optimization problem, a formulation that has several major benefits.³ By selecting total fuel consumption as the cost function, powered descent trajectories ensure fuel-optimality, in contrast to the polynomial method used on Mars Science Laboratory (MSL).⁴ Both control and path constraints can also be explicitly considered in a convex formulation, whereas in previous missions, constraints were satisfied by restricting admissible maneuvers to well-behaved and simple scenarios.⁵ Since a convex optimization program can be guaranteed to converge to the unique solution within a given accuracy in a finite number of iterations, it is suitable for onboard implementation. For these reasons, NASA has cited convex optimization as a potential next-generation solution for powered descent guidance for Mars missions.⁶

The convex programming approach, however, is based on a deterministic model of the dynamics of the powered descent phase of the mission, and therefore it is only designed to steer a single initial state to the target. In practice, the initial state is not a single point, but rather it is a random variable described by a distribution. Furthermore, if an unmodeled external force disturbs the spacecraft from its nominal trajectory, the deterministic guidance law includes no notion of how this disturbance will impact the final state. One solution to this problem is to continuously recompute, on-the-fly, a new optimal trajectory to be followed by the guidance subsystem. This method of closing the loop, while successful, is not explicitly included in the mathematical model of the guidance system. As a consequence, results from the analysis using the deterministic model, such as satisfaction of constraints, may not perform satisfactorily when applied to the real system.

With these limitations in mind, we propose in this paper a stochastic extension to the convex programming approach for PDG. The spacecraft's position and velocity is modeled as a normally distributed random

^{*}Ph.D. Candidate, Department of Aerospace Engineering, Georgia Institute of Technology, Atlanta, GA, 30332, USA.

[†]Dean's Professor, School of Aerospace Engineering, and Institute for Robotics and Intelligent Machines, Georgia Institute of Technology, Atlanta, GA, 30332, USA.

variable with Brownian motion process noise acting as an external disturbance force. The initial and target points from the deterministic case are generalized to initial and target normal distributions. We use recent results from stochastic optimal control theory, referred to as Covariance Steering (CS),^{7–11} to compute the required feedback of deviations from a reference trajectory to control the position and velocity covariances.

Two important physical constraints during powered descent are the minimum and maximum engine throttle limits. In a deterministic setting, it can be shown from the Minimum Principle that the fuel-optimal throttle setting is necessarily on either the minimum or maximum limit. If the state is, instead, a random variable, the closed-loop control becomes a random variable as well. The situation then becomes more complicated, since the statistics of the control variable depend on the reference (mean) control, the state covariance, and the feedback gain. This issue is addressed in this paper by setting reference control throttle bounds as a function of the closed-loop control covariance.

The organization of this paper is as follows. In Section II, we introduce a stochastic model for powered descent and show that, under certain assumptions, the dynamics can be separated into a deterministic mean component and a stochastic deviation from the mean. In Section III, we formulate the stochastic PDG problem, and then in Section IV, the probabilistic throttle constraint is analyzed and a conservative relaxation is proposed. We then review the problems of mean and covariance steering in Sections V.A and V.B. In Section V.C we extend the linear covariance steering theory to handle uncertain mass that enables a simple Covariance Steering Powered Descent Guidance (CS-PDG) algorithm suitable for onboard use, which is presented in Section V.D. Finally, this approach is demonstrated in a numerical simulation in Section VI.

A. Notation

Let $\|\cdot\|$ be the Euclidean norm on \mathbb{R}^n , and let $\mathsf{E}[f(x)]$ be the expectation of a function of a random variable x, and denote the mean of a random vector x by $\mathsf{E}[x] = \bar{x}$ and the difference from the mean as $\tilde{x} = x - \bar{x}$. We write the covariance of a normally distributed random vector x as $P_x = \mathsf{E}[\tilde{x}\tilde{x}^{\mathsf{T}}]$, and we write $x \sim \mathcal{N}(\bar{x}, P_x)$ to denote that x is normally distributed with mean \bar{x} and covariance P_x . For a square matrix A, we write $A > 0 \ (\geq 0)$ if A is positive (semi-)definite, i.e., $x^{\mathsf{T}}Ax > 0 \ (\geq 0)$ for all nonzero real vectors x.

II. System Model

Consider a spacecraft during powered descent modeled as a point-mass with position vector $r \in \mathbb{R}^3$ in a surface-fixed inertial frame. The spacecraft motion is modeled by the stochastic differential equation

$$d\dot{r} = (u/m + g)dt + (\gamma/m)dw, \tag{1}$$

$$\dot{m} = -\alpha \|u\|, \tag{2}$$

where m>0 is the spacecraft mass, $u\in\mathbb{R}^3$ is the control thrust, $g\in\mathbb{R}^3$ is the gravitational acceleration, and w is a three-dimensional standard Brownian motion scaled by $\gamma>0$. Let $x=(r,\dot{r})$, and assume that the initial state $x_0\sim\mathcal{N}(\bar{x}_0,P_{x_0})$ is a six-dimensional normally distributed random vector with known mean \bar{x}_0 and known covariance P_{x_0} . Assume that the initial mass $m_0>0$ is fixed and known. Furthermore, assume a given control structure so that at each time the control command is a function of a deterministic feedforward term and a feedback term that depends linearly on the deviation of x from the mean. By Jensen's inequality (Ref. 12, Thm. 7.44), we know that $\mathbb{E}(\|u\|) \geq \|\mathbb{E}(u)\| = \|\bar{u}\|$. Assuming that the mean control is much larger than the deviation we can approximate

$$\mathsf{E}(\|u\|) = \mathsf{E}(\|\bar{u} + \tilde{u}\|) \approx \|\bar{u}\|. \tag{3}$$

It then follows from Eq. (2) that the mass change is entirely due to the mean control, that is,

$$\dot{m} = -\alpha \|\bar{u}\|. \tag{4}$$

Since the initial mass is fixed, we conclude that the mass varies deterministically. The mean acceleration then satisfies the ordinary differential equation

$$\ddot{\bar{r}} = \bar{u}/m + g,\tag{5}$$

while the deviation from the mean is given by the stochastic differential equation

$$d\dot{\tilde{r}} = (\tilde{u}/m)dt + (\gamma/m)dw. \tag{6}$$

Assume, for the purposes of analyzing the perturbed system, that the mass is a fixed function of time. Let K = K(t) be a real-valued 3×6 time-varying gain matrix such that $\tilde{u} = K\tilde{x} = K(x - \bar{x})$. The perturbed system (6) can then be written as a linear time-varying stochastic differential equation (dropping explicit dependence on time for notational simplicity) as follows

$$d\tilde{x} = (A + B_m K)\tilde{x}dt + \gamma B_m dw, \tag{7}$$

where $B_m(t) = B/m(t)$ and

$$A = \begin{bmatrix} 0 & I \\ 0 & 0 \end{bmatrix}, \qquad B = \begin{bmatrix} 0 \\ I \end{bmatrix}. \tag{8}$$

Since \tilde{x}_0 is normally distributed with zero mean, and w is a standard Brownian motion, it follows from Eq. (7) that \tilde{x} is a zero-mean random process normally distributed with covariance matrix $P_x = \mathsf{E}[\tilde{x}\tilde{x}^{\dagger}]$, which satisfies the matrix differential equation

$$\dot{P}_x = (A + B_m K) P_x + P_x (A + B_m K)^{\mathsf{T}} + \gamma^2 B_m B_m^{\mathsf{T}}, \qquad P_x(0) = \mathsf{E}[\tilde{x}(0) \tilde{x}^{\mathsf{T}}(0)] = P_{x_0}. \tag{9}$$

It also follows from (7) that the feedback control $\tilde{u} = K\tilde{x}$ is a zero-mean random process with covariance

$$P_u = \mathsf{E}[\tilde{u}\tilde{u}^\mathsf{T}] = KP_xK^\mathsf{T}. \tag{10}$$

III. Problem Formulation

Our objective is to design a control pair (\bar{u}, K) that brings the spacecraft to a soft landing at the origin at a final time $t_f > 0$, which needs to be determined. Thus, we enforce the endpoint constraints on the mean and the covariance

$$\bar{x}(t_f) = 0, \qquad P_x(t_f) = P_{x_f},$$
(11)

where P_{x_f} is a fixed symmetric positive-definite matrix.

The mass is constrained from below by the dry mass $m_d > 0$ at all times. The glide slope θ_{gs} , which is the angle that the position vector makes with the vertical, is given as a function of the position as follows¹

$$\theta_{gs}(r) = \arctan\left(\frac{\sqrt{r_2^2 + r_3^2}}{r_1}\right),\tag{12}$$

where $r=(r_1,r_2,r_3)$ with r_1 is along the vertical upward direction, as shown in Figure 1. We constrain the mean glide slope $\theta_{gs}(\bar{r}) \leq \theta_{gs_0} \leq \pi/2$ by enforcing

$$||S_{qs}\bar{x}|| + c_{qs}^{\mathsf{T}}\bar{x} \le 0, \quad t \in [0, t_f],$$
 (13)

where

$$S_{gs} = \begin{bmatrix} 0 & 1 & 0 & 0 & 0 & 0 \\ 0 & 0 & 1 & 0 & 0 & 0 \end{bmatrix}, \quad c_{gs} = \begin{bmatrix} -\tan\theta_{gs_0} & 0 & 0 & 0 & 0 \end{bmatrix}^{\mathsf{T}}. \tag{14}$$

The angle the mean control vector \bar{u} makes with the vertical is constrained by a maximum pointing cone angle θ_{pc_0} via

$$\|\bar{u}\|\cos\theta_{pc_0} - e_1^{\mathsf{T}}\bar{u} \le 0, \quad t \in [0, t_f],$$
 (15)

where $e_1 = (1,0,0)^{\mathsf{T}}$. Let now $\rho_2 > \rho_1 > 0$ be fixed bounds on the control magnitude, and let the set

$$\Omega = \{ z \in \mathbb{R}^3 : \rho_1 \le ||z|| \le \rho_2 \}. \tag{16}$$

We wish to enforce the probability that the random vector u is not in Ω (i.e., the control u violates the magnitude constraints) be less than $\beta > 0$, that is,

$$\Pr(u \in \Omega) = \int_{\Omega} f(z, \bar{u}, P_u) dz \ge 1 - \beta \quad \text{for all } t \in [0, t_f],$$
(17)

where f is the 3-dimensional Gaussian probability density function given by

$$f(z, \bar{u}, P_u) = \frac{1}{(2\pi)^{3/2} (\det P_u)^{1/2}} \exp\left[-\frac{1}{2} (z - \bar{u})^{\mathsf{T}} P_u^{-1} (z - \bar{u})\right]. \tag{18}$$

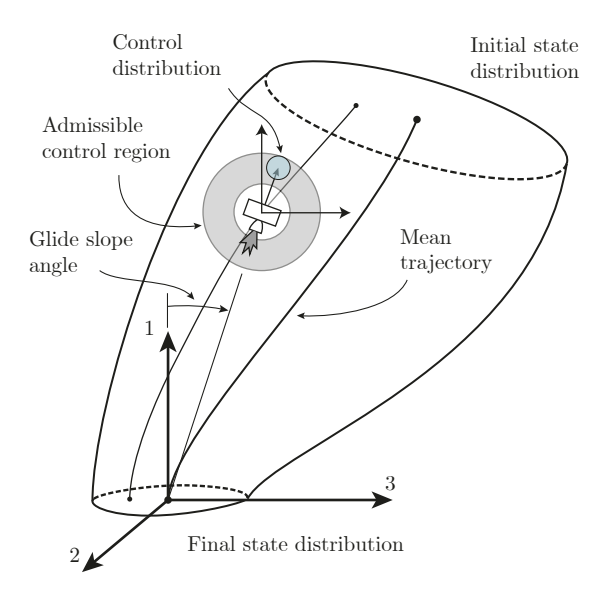


Figure 1: Powered descent with covariance control.

Subject to the above constraints, we wish to minimize the fuel cost of the mean control

$$J(\bar{u}) = \int_0^{t_f} \|\bar{u}(t)\| \, \mathrm{d}t,\tag{19}$$

by varying the mean (feedforward) control, the time-varying feedback gain matrix, and the final time. Formally stated, we want to solve the following problem, which we refer to as the *Stochastic Powered Descent Guidance Problem*:

$$\min_{\bar{u}, K, t_f} \int_0^{t_f} \|\bar{u}(t)\| \, \mathrm{d}t \tag{20a}$$

s.t.
$$\ddot{r} = \bar{u}/m + q$$
 (20b)

$$\dot{m} = -\alpha \|\bar{u}\| \tag{20c}$$

$$d\tilde{x} = (A + B_m K)\tilde{x}dt + \gamma B_m dw \tag{20d}$$

$$\bar{x}(0) = \bar{x}_0, \quad m(0) = m_0, \quad P_x(0) = P_{x_0}$$
 (20e)

$$\bar{x}(t_f) = 0, \quad P_x(t_f) = P_{x_f}$$
 (20f)

$$u = \bar{u} + K\tilde{x} \tag{20g}$$

$$m(t) \ge m_d$$
 for all $t \in [0, t_f]$ (20h)

$$||S_{gs}\bar{x}(t)|| - c_{gs}^{\mathsf{T}}\bar{x}(t) \le 0$$
 for all $t \in [0, t_f]$ (20i)

$$\|\bar{u}(t)\|\cos\theta_{pc_0} - e_1^{\mathsf{T}}\bar{u}(t) \le 0$$
 for all $t \in [0, t_f]$ (20j)

$$\Pr(u(t) \in \Omega) > 1 - \beta \qquad \text{for all } t \in [0, t_f]$$
 (20k)

Observe that we are only minimizing a deterministic objective function rather than minimizing a linear combination of the fuel cost and a penalty on the control covariance. We do this because the probabilistic constraint on the control (20k) introduces a natural coupling between the deterministic and stochastic problems. As it will be shown in Section A, in the absence of disturbances, the fuel optimal solution has the property that $u \in \partial \Omega$ for all time (i.e., the minimum-fuel optimal control problem is bang-bang), and therefore we adopt the heuristic that a good controller will allow the mean control to get as close to $\partial \Omega$ as possible, subject to the probabilistic constraint (20k). This notion is made more precise in Corollary V.2 below.

IV. Probabilistic Bound on Thrust

In the deterministic case, we constrain u to the set Ω by enforcing the 2-norm constraint

$$\rho_1 \le ||u|| \le \rho_2,\tag{21}$$

which permits us to use existing methods¹ to convexify and solve the powered descent problem numerically. Next, consider the stochastic case with a probabilistic constraint on the control. For a fixed covariance P_u , Eq. (17) is equivalent to constraining the mean control to a subset $\Omega_{\beta}^{P_u} \subseteq \Omega$, given by

$$\Omega_{\beta}^{P_u} = \{ \bar{u} \in \Omega : \int_{\Omega} f(z, \bar{u}, P_u) dz \ge 1 - \beta \}.$$
(22)

Define

$$\sigma^2 = \sigma_{\text{max}}^2(P_u),\tag{23}$$

where $\sigma_{\max}^2(P_u)$ denotes the maximum singular value of P_u . For simplicity, let Ω_{β}^{σ} denote $\Omega_{\beta}^{\sigma^2 I}$, and let the pair $(\rho_1^{\sigma}, \rho_2^{\sigma})$ be defined by

$$\rho_1^{\sigma} = \min\{\|\bar{u}\| : \bar{u} \in \Omega_{\beta}^{\sigma}\}, \qquad \rho_2^{\sigma} = \max\{\|\bar{u}\| : \bar{u} \in \Omega_{\beta}^{\sigma}\}. \tag{24}$$

The relationship between Ω , $\Omega_{\beta}^{P_u}$, and Ω_{β}^{σ} is illustrated in Figure 2.

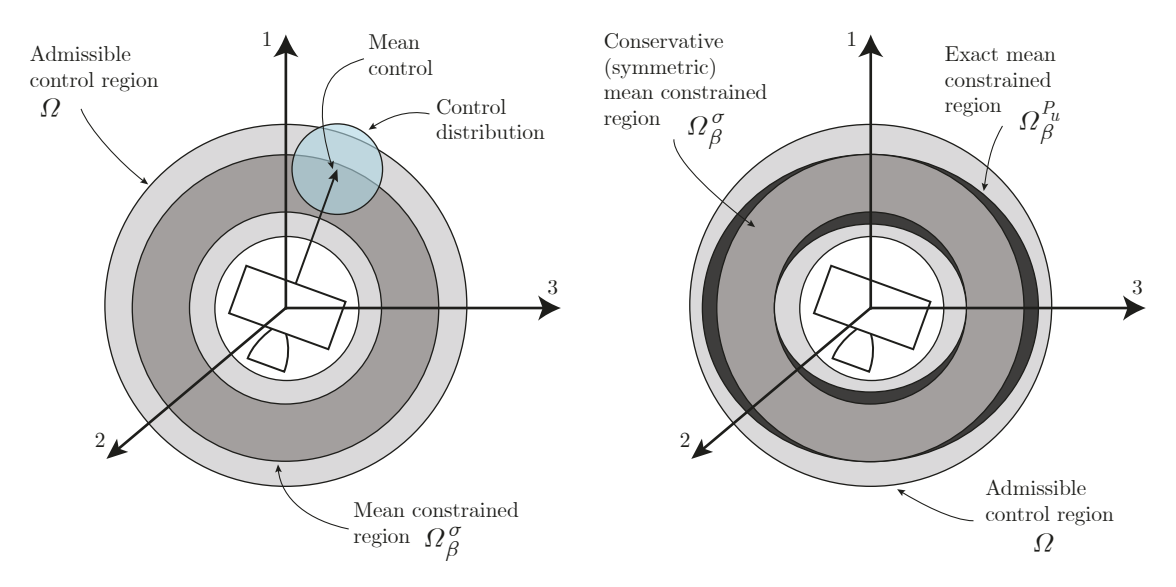


Figure 2: Left, two-dimensional view of admissible thrust region Ω and the derived mean constrained region Ω_{β}^{σ} . Right, comparison of exact mean constrained region $\Omega_{\beta}^{P_u}$ and conservative mean constrained region Ω_{β}^{σ} .

For $P_u = \sigma^2 I$, the Gaussian probability density function $f(z, \bar{u}, \sigma^2 I)$ satisfies

$$\int_{\Omega} f(z, u_1, \sigma^2 I) \, dz = \int_{\Omega} f(z, u_2, \sigma^2 I) \, dz, \quad \text{for} \quad ||u_1|| = ||u_2||.$$
 (25)

Let the polar coordinate system (s, θ, ϕ) defined in Figure 3 and let the integration variable $z = z(s, \theta, \phi)$, where s = ||z||. It follows from Eq. (25) that, for the covariance matrix $\sigma^2 I$, the Gaussian probability density function can be equivalently stated in polar coordinates as

$$f_s(z(s,\theta,\phi),\rho,\sigma^2) = \frac{1}{(2\pi)^{3/2}\sigma^3} \exp\left[\frac{-(s^2 - 2s\rho\cos\theta + \rho^2)}{2\sigma^2}\right],$$
 (26)

where ρ is the radial distance of the mean from the origin along the z axis. Integrated over Ω , this function admits the solution in terms of the error function

$$\int_{\Omega} f_s(z, \rho, \sigma^2) dz = \frac{\sigma}{\sqrt{2\pi}\rho} \left[\exp\left[\frac{-(\rho_1 - \rho)^2}{2\sigma^2} \right] - \exp\left[\frac{-(\rho_2 - \rho)^2}{2\sigma^2} \right] - \exp\left[\frac{-(\rho_1 + \rho)^2}{2\sigma^2} \right] + \exp\left[\frac{-(\rho_2 + \rho)^2}{2\sigma^2} \right] \right] + \exp\left[\frac{-(\rho_2 + \rho)^2}{2\sigma^2} \right] + \exp\left[\frac{-(\rho_2 +$$

Using Eq. (27) we can easily compute ρ_1^{σ} and ρ_2^{σ} since, from Eq. (25),

$$\{\|u\| : u \in \Omega_{\beta}^{\sigma}\} = \{\rho \in [\rho_1, \rho_2] : \int_{\Omega} f_s(z, \rho, \sigma^2) \, \mathrm{d}z \ge 1 - \beta\}.$$
 (28)

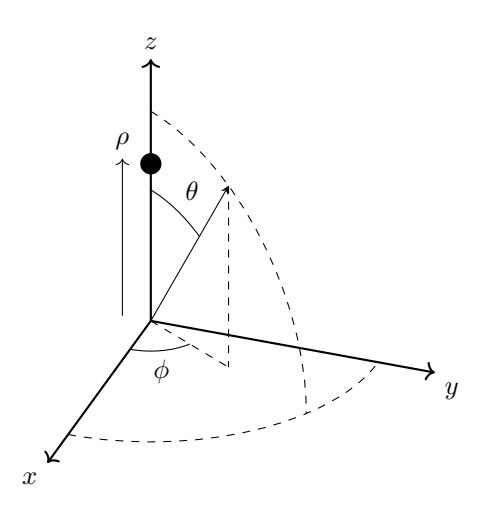


Figure 3: Polar coordinate system description.

Note that for σ^2 large enough, Ω_{β}^{σ} may be empty and therefore $(\rho_1^{\sigma}, \rho_2^{\sigma})$ may not be defined. However, we have made the assumption that the uncertainty in the control will be relatively small compared to the mean control, so we will also assume that the new thrust bounds are always defined. Finally, the probabilistic constraint (17) is conservatively restated in the desired form as

$$\rho_1^{\sigma}(t) \le \|\bar{u}(t)\| \le \rho_2^{\sigma}(t) \quad \text{for all } t \in [0, t_f],$$
 (29)

where ρ_1^{σ} and ρ_2^{σ} as in (24).

V. Mean and Covariance Steering

A. Mean Steering

For the purposes of mean steering, assume that P_u and β are fixed, and hence ρ_1^{σ} , ρ_2^{σ} are also fixed. The mean steering component of the PDG problem (20) thus reduces to the deterministic PDG problem by

substituting Eq. (30i) in lieu of the probabilistic constraint (20k):

$$\bar{J}_{\rho_1^{\sigma}, \rho_2^{\sigma}}^* = \min_{\bar{u}, t_f} \quad \bar{J}_{\rho_1^{\sigma}, \rho_2^{\sigma}}(\bar{u}; t_f) = \int_0^{t_f} \|\bar{u}(t)\| \, \mathrm{d}t$$
 (30a)

s.t.
$$\ddot{r} = \bar{u}/m + g$$
 (30b)

$$\dot{m} = -\alpha \|\bar{u}\| \tag{30c}$$

$$\bar{r}(0) = \bar{r}_0, \ \dot{\bar{r}}(0) = \dot{\bar{r}}_0, \ m(0) = m_0$$
 (30d)

$$\bar{r}(t_f) = 0, \ \dot{\bar{r}}(t_f) = 0$$
 (30e)

$$m(t) \ge m_d$$
 for all $t \in [0, t_f]$ (30f)

$$||S_{as}\bar{x}(t)|| - c_{as}^{\mathsf{T}}\bar{x}(t) \le 0 \qquad \text{for all } t \in [0, t_f]$$

$$||S_{gs}\bar{x}(t)|| - c_{gs}^{\mathsf{T}}\bar{x}(t) \le 0 \qquad \text{for all } t \in [0, t_f] \qquad (30g)$$

$$||\bar{u}(t)|| \cos \theta_{pc_0} - e_1^{\mathsf{T}}\bar{u}(t) \le 0 \qquad \text{for all } t \in [0, t_f] \qquad (30h)$$

$$\rho_1^{\sigma}(t) \le ||\bar{u}(t)|| \le \rho_2^{\sigma}(t) \qquad \text{for all } t \in [0, t_f] \qquad (30i)$$

$$\rho_1^{\sigma}(t) \le \|\bar{u}(t)\| \le \rho_2^{\sigma}(t) \qquad \text{for all } t \in [0, t_f]$$
(30i)

This problem has been extensively studied in the literature, 1,2,13 where it has been shown that the solution has a max-min-max control structure without singular arcs. While this problem has been studied with the assumption of constant thrust bounds, it turns out that this property also holds for time-varying bounds. This result is formally stated in the following theorem.

Theorem V.1. The optimal thrust profile \bar{u}^* solving the PDG problem (30) has a max-min-max structure with no singular arcs. That is,

$$\|\bar{u}^*(t)\| = \begin{cases} \rho_2^{\sigma}(t), & 0 \le t \le t_1, \\ \rho_1^{\sigma}(t), & t_1 < t \le t_2, \\ \rho_2^{\sigma}(t), & t_2 < t \le t_f, \end{cases}$$
(31)

for all $t \in [0, t_f^*]$, where t_f^* is the optimal final time.

We refer the reader to Ref. 1 for a proof of the special case of constant throttle bounds. However, the argument is based on the pointwise Minimum Principle and therefore works for time-varying bounds. We use "cost with the bounds (ρ_1, ρ_2) " to refer to the minimum cost of problem (30) when computed with (ρ_1, ρ_2) substituted into Eq. (30i). The following corollary is a direct consequence of the Minimum Principle.

Corollary V.2. Let the functions ρ_1^1 , ρ_2^1 , ρ_1^2 , and ρ_2^2 be piecewise continuous, positive functions defined over the interval $[0,\infty)$, where

$$\rho_1^1(t) < \rho_1^2(t) < \rho_2^2(t) < \rho_2^1(t) \quad \text{for all } t \in [0, \infty).$$
 (32)

Then

$$\bar{J}_{\rho_1^1,\rho_2^1}^* < \bar{J}_{\rho_1^2,\rho_2^2}^*. \tag{33}$$

Proof. Assume, to the contrary, that $\bar{J}_{\rho_1^1,\rho_2^1}^* \geq \bar{J}_{\rho_1^2,\rho_2^2}^*$, and let $(\bar{u}^{*2},t_f^{*2}) = \arg\min \bar{J}_{\rho_1^2,\rho_2^2}(\bar{u};t_f)$. Since $\rho_1^1(t) < \rho_1^2(t)$ and $\rho_2^2(t) < \rho_2^1(t)$ for all time, the control \bar{u}^{*2} is within the bounds (ρ_1^1,ρ_2^1) . This implies that $\bar{J}_{\rho_1^1,\rho_2^1}^*$ cannot be greater than $\bar{J}^*_{\rho_1^2,\rho_2^2}$, since the throttle constraint defined by ρ_1^1 and ρ_2^1 is a relaxation from ρ_1^2 and ρ_2^2 . It follows that \bar{u}^{*2} is an optimal control for the problem with bounds (ρ_1^1,ρ_2^1) . However, $\rho_1^1(t) < \|\bar{u}^{*2}(t)\| < \rho_2^1(t)$ at every instant of time, contradicting Theorem V.1. Therefore $\bar{J}^*_{\rho_1^1,\rho_2^1} \neq \bar{J}^*_{\rho_1^2,\rho_2^2}$, and we conclude that $\bar{J}_{\rho_{1}^{1},\rho_{2}^{1}}^{*} < \bar{J}_{\rho_{1}^{2},\rho_{2}^{2}}^{*}$

Corollary V.2 makes explicit the trade-off between robustness and fuel-optimality. If there is any interval of time during which the control magnitude bound is relaxed, there will necessarily be a corresponding decrease in fuel required for an optimal trajectory. On the other hand, there will be external disturbances, variations in system performance, and other forms of uncertainty that may cause the spacecraft to deviate from the reference trajectory, which must be corrected though feedback. We are therefore motivated to study how uncertainty affects the feedback control, and how to design minimum-fuel trajectories, while respecting the expectation that the feedback control will be used to correct for uncertainty and external disturbances.

B. Covariance Steering

As shown in the previous section, the fuel cost of the deterministic PDG problem decreases as the thrust bounds are relaxed. Together with the observation that the thrust bounds ρ_1^{σ} and ρ_2^{σ} approach their limits ρ_1 and ρ_2 as the control covariance decreases, this fact motivates us to design a feedback controller so that the control covariance is minimized.

1. Motivating Example

In order to demonstrate the relationship of the closed-loop state covariance on the control covariance, we consider the one-dimensional closed-loop stochastic system

$$dy = (a - bk)y dt + c dv, (34)$$

where a, b, c are fixed scalars, y is the state, k is a feedback gain, and v is a one-dimensional standard Brownian motion. Let p be the variance of y, that is, $p = \mathsf{E}(y^2)$, then

$$\dot{p} = 2(a - bk)p + c^2. \tag{35}$$

Suppose that we are interested in finding a gain that maintains a fixed state variance (a problem referred to as covariance assignment). Solving for k when $\dot{p} = 0$, we obtain the gain k_s as a function of the constant state variance p_s

$$k_s = \frac{1}{b} \left(a + \frac{c^2}{2p_s} \right),\tag{36}$$

and the corresponding control variance is $k_s^2 p_s$. Intuitively, the state variance decreases to zero as the gain increases to infinity, however, this is not the case for the control variance. Taking the derivative of the control variance with respect to the state variance we find that

$$\frac{\mathrm{d}(k_s^2 p_s)}{\mathrm{d}p_s} = \frac{a^2 - c^4 / 4p_s^2}{b^2},\tag{37}$$

and therefore the control variance is minimized at $p_{s,\min} = c^2/2 |a|$. The values of k_s and $k_s^2 p_s$ for a, b, c = 1 are given in Figure 4, which compares the state variance and the control variance as the gain is increased. In the previous sections, we have shown that as the control covariance decreases, the mean control can be set closer to the fuel-optimal value while still satisfying probabilistic constraints. And in this example we see that, at least in the single dimensional case, there is a minimum control variance.

Returning to the powered descent problem, we are interested in enforcing endpoint constraints on the state covariance rather than steady-state requirements, as was done in the previous example. Similarly, since the powered descent problem has finite time horizon, the integral of the control covariance will be minimized rather than the steady-state control control variance. The minimum control covariance will, in turn, maximize the mean control constraint set Ω^{σ}_{β} , which, by Corollary V.2, will minimize the fuel required to solve the deterministic PDG problem (30).

2. Finite Horizon Covariance Steering

Consider the stochastic system (7) with initial covariance P_{x_0} at time t = 0. Let $t_f > 0$ be fixed. We want to find a gain matrix K(t) for $t \in [0, t_f]$ such that the state covariance in Eq. (9) is equal to P_{x_f} at time $t = t_f$ while minimizing the functional

$$\tilde{J}(\tilde{u}) = \mathsf{E} \int_0^{t_f} \left(\tilde{u}^\mathsf{T}(t) Q_u(t) \tilde{u}(t) + \tilde{x}^\mathsf{T}(t) Q_x(t) \tilde{x}(t) \right) \mathrm{d}t = \int_0^{t_f} \left(\operatorname{tr} Q_u(t) P_u(t) + \operatorname{tr} Q_x(t) P_x(t) \right) \mathrm{d}t, \tag{38}$$

where $Q_u(t)$ is a positive definite control effort weighting matrix and $Q_x(t)$ is a non-negative definite state error weight matrix for all $t \in [0, t_f]$. This problem, which is referred to as the Covariance Steering (CS) problem, can be formally stated as follows

$$\min_{K} \quad \int_{0}^{t_f} \operatorname{tr} Q_u K P_x K^{\mathsf{T}} + \operatorname{tr} Q_x P_x \, \mathrm{d}t \tag{39a}$$

s.t.
$$\dot{P}_x = (A + B_m K) P_x + P_x (A + B_m K)^{\mathsf{T}} + \gamma^2 B_m B_m^{\mathsf{T}}$$
 (39b)

$$P_x(0) = P_{x_0}, \quad P_x(t_f) = P_{x_f}$$
 (39c)

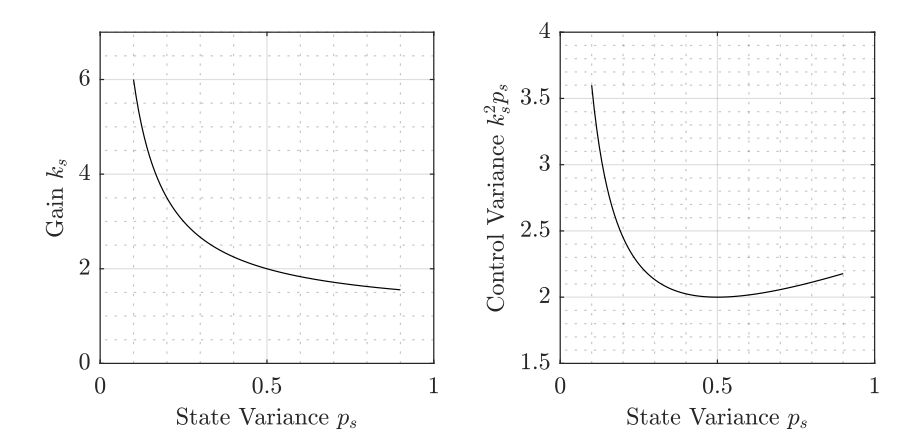


Figure 4: Steady state variances for a, b, c = 1.

This problem has been studied in Refs. 8–10, where it was shown that if the pair (A, B_m) is controllable, then there exists a feedback gain K(t) that takes any initial covariance P_{x_0} to a final covariance P_{x_f} in finite time. Furthermore, a closed-form solution to the above problem was given in Ref. 10, which for completeness we present below.

Theorem V.3. [10] The covariance steering problem in continuous time (39) has the solution

$$K(t) = -Q_u^{-1}(t)B_m^{\mathsf{T}}\Pi(t), \tag{40}$$

where $\Pi(t)$ is a symmetric matrix that satisfies the matrix Riccati equation

$$-\dot{\Pi} = A^{\mathsf{T}}\Pi + \Pi A + Q_x(t) - \Pi B_m Q_y^{-1}(t) B_m^{\mathsf{T}}\Pi, \tag{41}$$

with the initial condition

$$\Pi(0) = \frac{\gamma^2 P_{x_0}^{-1}}{2} - \Phi_{12}^{-1} \Phi_{11} - P_{x_0}^{-1/2} \left(\frac{\gamma^4 I}{4} + P_{x_0}^{1/2} \Phi_{12}^{-1} P_{x_f} \Phi_{12}^{-\tau} P_{x_0}^{1/2} \right)^{1/2} P_{x_0}^{-1/2}, \tag{42}$$

where

$$\begin{bmatrix} \Phi_{11} & \Phi_{12} \\ \Phi_{21} & \Phi_{22} \end{bmatrix} = \begin{bmatrix} \Phi_{11}(t_f, 0) & \Phi_{12}(t_f, 0) \\ \Phi_{21}(t_f, 0) & \Phi_{22}(t_f, 0) \end{bmatrix}, \tag{43}$$

and where

$$\Phi(t,s) = \begin{bmatrix} \Phi_{11}(t,s) & \Phi_{12}(t,s) \\ \Phi_{21}(t,s) & \Phi_{22}(t,s) \end{bmatrix}$$
(44)

is the transition matrix for the Hamiltonian system where

$$\frac{\partial \Phi(t,s)}{\partial t} = \mathcal{H}(t)\Phi(t,s), \quad \Phi(s,s) = I, \tag{45}$$

$$\mathcal{H}(t) = \begin{bmatrix} A & -B_m Q_u^{-1}(t) B_m^{\mathsf{T}} \\ -Q_x(t) & -A^{\mathsf{T}} \end{bmatrix}. \tag{46}$$

C. Covariance Steering with Mass Feedback

In Section V.A, we assumed that the state and control covariances were known before solving the mean steering problem. However, the covariance steering solution presented in the previous section depends on the mass, which, in turn, is an output from the solution of the mean steering problem. Therefore, a control that solves the mean and covariance steering problems cannot be found by simply solving each problem separately. One solution would be to perform a fixed point iteration until the mean and covariance steering

solutions are in agreement, as was done in [14], but such an iteration would be time consuming and would require guarantees on convergence to be suitable for onboard use. In this section, we present an alternate approach: we modify the covariance steering problem so that it does not depend on the mass.

Since the throttle is bounded by ρ_1 and ρ_2 , the mass will also be bounded from below by m_ℓ and from above by m_u , where

$$m_{\ell}(t) = m_0 - \rho_2 \alpha t,\tag{47}$$

$$m_u(t) = m_0 - \rho_1 \alpha t. \tag{48}$$

Let (K^{ℓ}, P_x^{ℓ}) be the solution of Problem (39) for $m = m_{\ell}$. Then P_x^{ℓ} solves

$$\dot{P}_x^{\ell} = (A + m_{\ell}^{-1} B K^{\ell}) P_x^{\ell} + P_x^{\ell} (A + m_{\ell}^{-1} B K^{\ell})^{\mathsf{T}} + \gamma^2 m_{\ell}^{-2} B B^{\mathsf{T}}, \quad P_x^{\ell}(0) = P_{x_0}, \tag{49}$$

with $P_x^{\ell}(t_f) = P_{x_f}$. Our objective is to augment this solution to solve the problem for any mass greater than m_{ℓ} , that is, we want to find K as a function of m, m_{ℓ} , and K^{ℓ} so that the state covariance is less than or equal to P_x^{ℓ} . Then, even when we only are given bounds on the mass, we can still ensure that

$$P_x(t_f) \le P_x^{\ell}(t_f) = P_{x_f}. \tag{50}$$

Proposition V.4. Let $P_x(0) = P_x^{\ell}(0)$ and

$$K(t,m) = \frac{m}{m_{\ell}(t)} K^{\ell}(t), \quad t \in [0, t_f].$$
 (51)

Then $P_x(t) \leq P_x^{\ell}(t)$ for all $t \in [0, t_f]$.

In order to prove this result we will need the following result from Ref. 15, which is restated as Lemma V.5 below and is adapted for our purposes in Corollary V.6.

Lemma V.5. [15] Let K_i , i = 1, 2, be a solution of

$$\dot{K}_{i} = -A_{i}^{\mathsf{T}}(t)K - KA_{i}(t) - Q_{i}(t) + KS_{i}(t)K \tag{52}$$

on some interval $\mathscr{T} \subseteq \mathbb{R}$. If for some $t_f \in \mathscr{T}$, $K_1(t_f) \leq K_2(t_f)$ or $(K_1(t_f) < K_2(t_f))$ and if

$$\begin{bmatrix} Q_2 & A_2^{\mathsf{T}} \\ A_2 & -S_2 \end{bmatrix} (t) \ge \begin{bmatrix} Q_1 & A_1^{\mathsf{T}} \\ A_1 & -S_1 \end{bmatrix} (t) \quad \text{for } t \in \mathscr{T}$$
 (53)

then $K_1(t) \leq K_2(t)$ or $(K_1(t) < K_2(t))$, respectively, for all $t \in \mathcal{F} \cap (-\infty, t_f]$.

Corollary V.6. Let P_i , i = 1, 2, be a solution of

$$\dot{P}_i = \mathcal{A}_i^{\mathsf{T}}(t)P_i + P_i\mathcal{A}_i(t) + \mathcal{Q}_i(t) \tag{54}$$

on the interval $[0, t_f]$. If $P_1(0) = P_2(0)$, and if

$$\begin{bmatrix} \mathcal{Q}_1 - \mathcal{Q}_2 & \mathcal{A}_1 - \mathcal{A}_2 \\ (\mathcal{A}_1 - \mathcal{A}_2)^\mathsf{T} & 0 \end{bmatrix} (t) \ge 0, \quad t \in [0, t_f],$$
 (55)

then $P_2(t) \leq P_1(t)$ for all $t \in [0, t_f]$.

Proof. Suppose that Eq. (53) holds. It follows from Lemma V.5,

$$K_1(t_f) \le K_2(t_f) \implies K_1(t) \le K_2(t) \quad \text{for all } t \in \mathcal{T} \cap (-\infty, t_f].$$
 (56)

This statement is equivalent to the statement

$$K_2(0) \le K_1(0) \implies K_2(t) \le K_1(t) \quad \text{for all } t \in \mathcal{T} \cap [0, \infty).$$
 (57)

The result follows by changing the sign of coefficients from Lemma V.5 accordingly.

Proof. (of Proposition V.4) Rewrite the equation for \dot{P}_x^{ℓ} as

$$\dot{P}_{x}^{\ell} = (A + m_{\ell}^{-1}BK^{\ell})P_{x}^{\ell} + P_{x}^{\ell}(A + m_{\ell}^{-1}BK^{\ell})^{\mathsf{T}} + \gamma^{2}m_{\ell}^{-2}BB^{\mathsf{T}}$$
(58)

$$= m_{\ell}^{-2} \left[(m_{\ell}^{2} A - m_{\ell} B K^{\ell}) P_{x}^{\ell} + P_{x}^{\ell} (m_{\ell}^{2} A - m_{\ell} B K^{\ell})^{\mathsf{T}} + \gamma^{2} B B^{\mathsf{T}} \right]. \tag{59}$$

Substituting $K = mK^{\ell}/m_{\ell}$ into the equation for \dot{P}_x yields

$$\dot{P}_x = (A + m^{-1}BK)P_x + P_x(A + m^{-1}BK)^{\mathsf{T}} + \gamma^2 m^{-2}BB^{\mathsf{T}}$$
(60)

$$= m_{\ell}^{-2} \left[(m_{\ell}^2 A - m_{\ell} B K^{\ell}) P_x + P_x (m_{\ell}^2 A - m_{\ell} B K^{\ell})^{\mathsf{T}} + \gamma^2 \frac{m_{\ell}^2}{m^2} B B^{\mathsf{T}} \right]. \tag{61}$$

Define

$$A_1 = A_2 = m_\ell^2 A - BK^\ell, \quad Q_1 = \gamma^2 BB^\mathsf{T}, \quad Q_2 = \gamma^2 \frac{m_\ell^2}{m^2} BB^\mathsf{T},$$
 (62)

so that

$$\dot{P}_x^{\ell} = m_{\ell}^{-2} (\mathcal{A}_1 P_x^{\ell} + P_x^{\ell} \mathcal{A}_1^{\mathsf{T}} + \mathcal{Q}_1), \tag{63}$$

$$\dot{P}_x = m_{\ell}^{-2} (\mathcal{A}_2 P_x + P_x \mathcal{A}_2^{\mathsf{T}} + \mathcal{Q}_2). \tag{64}$$

By Corollary V.6 with $P_1 = P_x^{\ell}$ and $P_2 = P_x$, if

$$\begin{bmatrix} Q_1 - Q_2 & 0 \\ 0 & 0 \end{bmatrix} (t) \ge 0, \quad t \in [0, t_f], \tag{65}$$

then $P_x(t) \leq P_x^{\ell}(t)$ for all $t \in [0, t_f]$. Since $m \geq m_{\ell}$ and $BB^{\mathsf{T}} \geq 0$,

$$\mathcal{Q}_1 - \mathcal{Q}_2 = \gamma^2 B B^{\mathsf{T}} \left(1 - \frac{m_\ell^2}{m^2} \right) \ge 0, \tag{66}$$

which implies that Eq. (65) holds, thus completing the proof.

A feedback gain determined using this procedure will depend on the mass, and therefore the control covariance will depend on the mass as well. To guarantee that the results of Section IV hold for any $m_{\ell} \leq m \leq m_u$, we must find an upper bound on P_u . To this end, let (K^{ℓ}, P_x^{ℓ}) be the solution of the covariance steering problem for $m(t) = m_{\ell}(t)$. Then

$$P_{u} = K P_{x} K^{\mathsf{T}} = \frac{m^{2}}{m_{\ell}^{2}} K^{\ell} P_{x} K^{\ell^{\mathsf{T}}} \le \frac{m_{u}^{2}}{m_{\ell}^{2}} K^{\ell} P_{x}^{\ell} K^{\ell^{\mathsf{T}}} = P_{u, \max}, \tag{67}$$

where the resulting upper bound $P_{u,\text{max}}$ is only a function of time. Interestingly, if the mass is known precisely when solving the covariance steering problem, then $m_u = m = m_\ell$, and it follows that $P_u = P_{u,\text{max}}$. More generally, the difference between P_u and $P_{u,\text{max}}$ decreases monotonically as the gap between the lower and upper bounds on mass decreases.

D. CS-PDG Algorithm

The results of this paper are summarized in the following algorithm for powered descent guidance.

Fixed Final Time CS-PSG Algorithm

- 1) Input $t_f, m_0, \beta, \gamma > 0, P_{x_0}, P_{x_f} > 0, \bar{x}_0, \text{ and } m_{\ell}(t), m_u(t) \text{ for } t \in [0, t_f].$
- 2) Solve the CS problem (39) with mass m_{ℓ} to obtain $P_{\tau}^{\ell}(t)$ and $K^{\ell}(t)$ for $t \in [0, t_f]$.
- 3) Set $K(t,m) = mK^{\ell}(t)/m_{\ell}(t)$.
- 4) Use $P_{u,\max}(t)$ from (67) to solve (24) for $\rho_1^{\sigma}(t)$ and $\rho_2^{\sigma}(t)$, $t \in [0, t_f]$.

- 5) Solve the deterministic PDG problem (30) for fixed t_f to obtain $\bar{u}(t)$ and $\bar{x}(t)$, $t \in [0, t_f]$.
- 6) Return control law $u(t, x, m) = \bar{u}(t) + K(t, m)(x \bar{x}(t))$.

The fuel cost is a unimodal function of final time,^{1,2} and therefore the free final time problem can be solved by performing a line search over t_f . Also, since the deterministic PDG problem returns an estimate for m(t), we can iteratively tighten the mass bounds $m_{\ell}(t), m_u(t)$. However, we found that this does not significantly improve performance, and problems arise from the discontinuous nature of the mean control that affects convergence. Furthermore, the feedback control will cause the actual mass to deviate slightly from the mass profile returned by the deterministic PDG solver, and by using hard lower and upper mass limits $m_{\ell}(t), m_u(t)$ the final covariance is guaranteed to be less than or equal to the target covariance by Theorem V.4.

VI. Numerical Simulation

In this section we present a numerical example of a powered divert maneuver for MSL. Suppose that the 1,905 kg MSL descent stage is at an altitude of 1,500 m with a velocity of 125 m/s and flight path angle of -36.9° when the target landing point is updated to a position 2,000 m behind the current position, in the plane of the velocity vector. Assume an initial state covariance of

$$P_{x_0} = \operatorname{diag}(200, 200, 200, 10, 10, 10), \tag{68}$$

and target final covariance

$$P_{x_f} = \text{diag}(10, 10, 10, 1, 1, 1), \tag{69}$$

where velocity and distance are in units of m/s and m. We enforce that the probability of an out of bounds throttle command is 0.1% ($\beta = 0.001$). Properties of the MSL descent stage and a summary of simulation settings are given in Table 1.

The optimal maneuver time was 88 sec, and select trials from a 2,000 trial Monte Carlo run are shown in Figures 5 and 6. In Figure 7 the control components from the Monte Carlo trials are shown relative to the maximum and minimum throttle constraints with 99.9% of trials contained within the blue tube. In this figure, we see that the tube representing a fixed probability of controls is along the constraint boundary. This is analogous to the deterministic case, where, instead, the known control would be on the constraint boundary.

The thrust magnitude profile is shown in Figure 8 next to a plot of the probability that u is in Ω as a function of the throttle percentage. The control covariance was higher at time t=1 than at time t=50, and hence the points where the probability curve intersects the line $1-\beta$ are closer together at t=1 than at t=50.

In addition to using the proposed method, this scenario was also run with three levels of constant throttle bounds (i.e., ρ_1^{σ} , ρ_2^{σ} constant) and the same feedback controller: the bounds were set so that the probabilistic constraint in control is satisfied at every instant of time; the bounds were manually tuned so that the maneuver appeared to be successful based on the Monte Carlo results; and the bounds were set to exactly the maximum and minimum limits. Lastly, the proposed method was also run with $\beta = 0.05$. A comparison of the proposed method to these four cases is shown in Figure 9, and numerical results are listed in Table 2.

As expected, the final state covariance in the large margin case meets the final covariance target, but uses more fuel compared to the proposed method. The case without any margin does not meet the final covariance target, but uses less fuel. Interestingly, when the margin was tuned so that the final covariance is nearly met, despite significant throttle saturation, there was a lower fuel cost compared to the proposed method. However, since the control is saturated, the state covariance dynamics in Eq. (9) no longer apply, and therefore the state statistics guaranteed by the covariance steering controller are no longer exact.

VII. Conclusion

In this paper, we have extended the deterministic theory on minimum-fuel powered descent to the more general case of steering the initial position and velocity distributions to a target position and velocity distributions, while considering Brownian motion process noise acting on the system. By assuming that the reference control is much larger than the deviation to correct for disturbances, we separated the stochastic

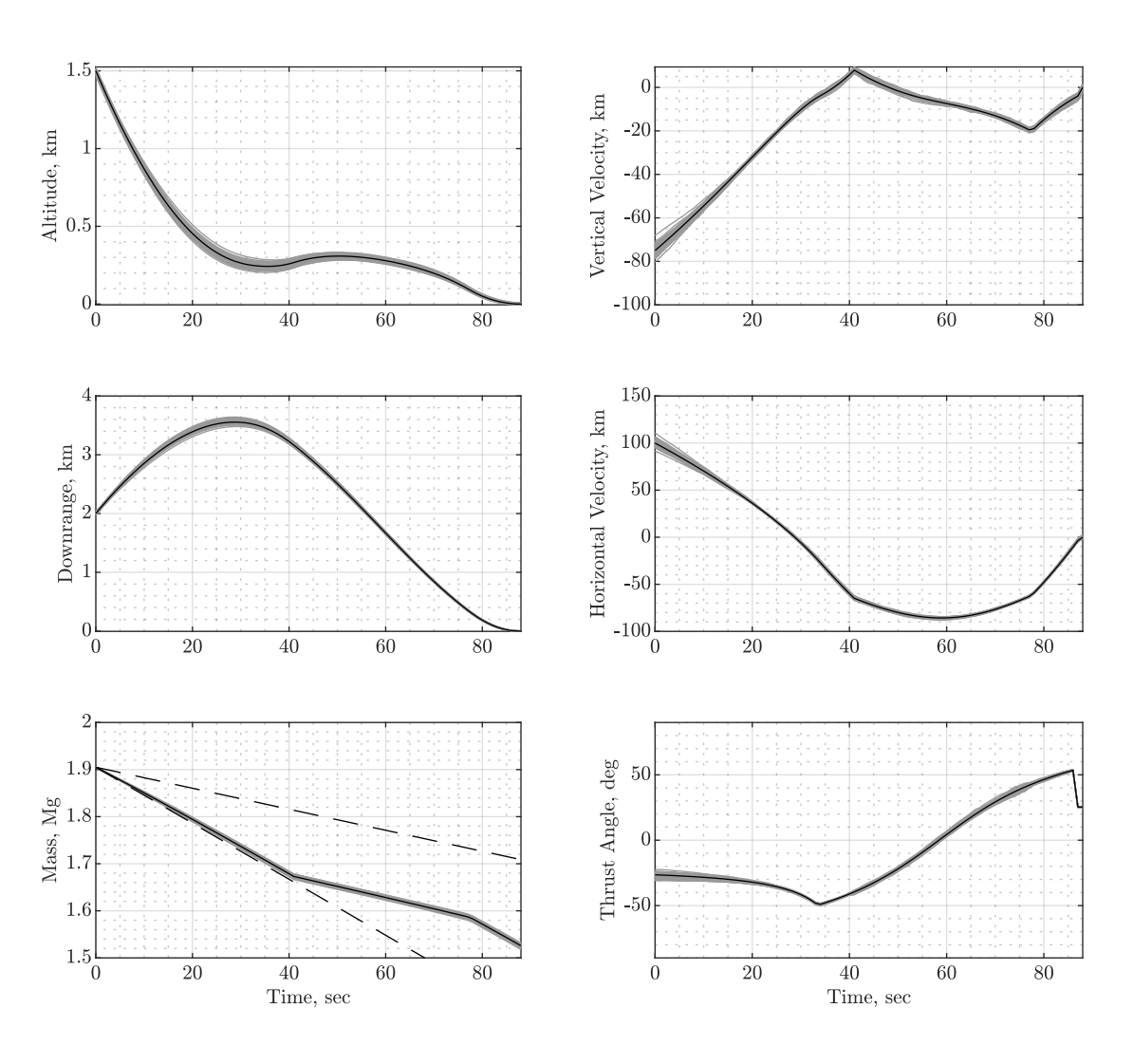


Figure 5: Select trajectories from a Monte Carlo simulation. The reference trajectory is depicted by a solid black line and trials are in gray. The thrust angle is measured from the vertical, and the minimum and maximum mass are plotted with dashed lines.

Table 1: Simulation settings

Property	Value	Unit	Property	Value	Unit
Number engines	6		Wet mass m_0	1,905	kg
Engine cant angle	27	\deg	Propellant mass	400	kg
Thrust per engine	3,100	N	α	4.4865 e-04	kg/N sec
Specific impulse	210	sec	P_{x_0}	$\mathrm{diag}(200, 200, 200, 10, 10, 10)$	m^2/s^2 , m^2
Total thrust	$16,\!573$	N	P_{x_f}	diag(10, 10, 10, 1, 1, 1)	m^2/s^2 , m^2
Minimum throttle	30	%	$ar{r}_0$	(1500, 0, 2000)	m
Maximum throttle	80	%	$\dot{ar{r}}_0$	(-75, 0, 100)	m/s
Pointing angle θ_{pc_0}	75	\deg			
Glide slope angle θ_{gs_0}	86	deg			

Table 2: Comparison of simulation results. The state covariance matrix was computed from 2,000 Monte Carlo runs, where position and velocity are in units of m and m/s, and the error is measured with the Frobenius norm. Note that if $\lambda_{min}(P_{x_f} - P_x(t_f)) < 0$, then $P_x(t_f) > P_{x_f}$.

	Propellant	Used, kg	Final Covariance Error		
	Reference	Mean	$ P_{x_f} - P_x(t_f) $	$\lambda_{\min}(P_{x_f} - P_x(t_f))$	
No margin	355.56	357.09	31.33	-31.33	
Small margin	367.96	367.76	17.82	-17.82	
Large margin	400.28	400.14	14.29	-14.29	
Proposed ($\beta = 0.001$)	379.17	379.70	2.29	-0.0019	
Proposed ($\beta = 0.05$)	366.54	367.18	1.61	-0.6315	

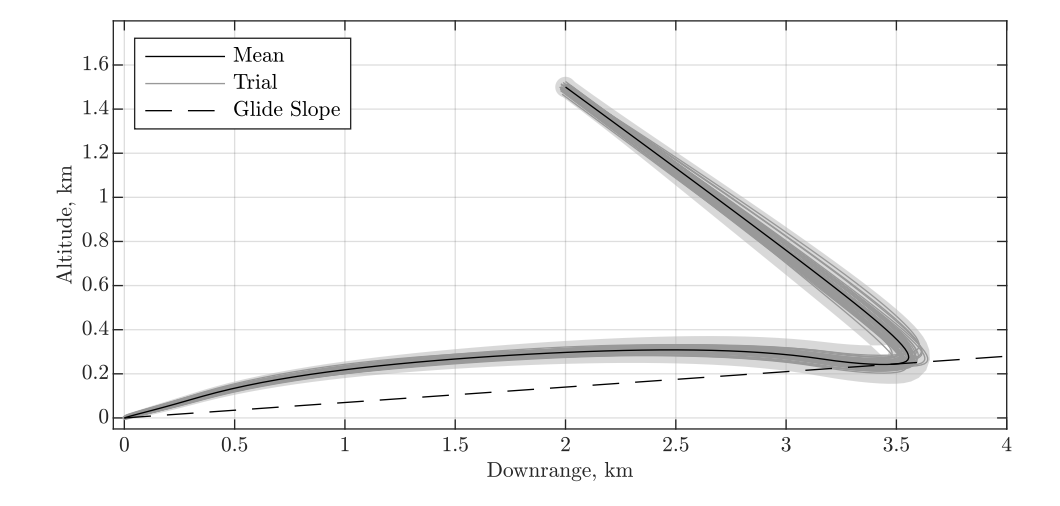
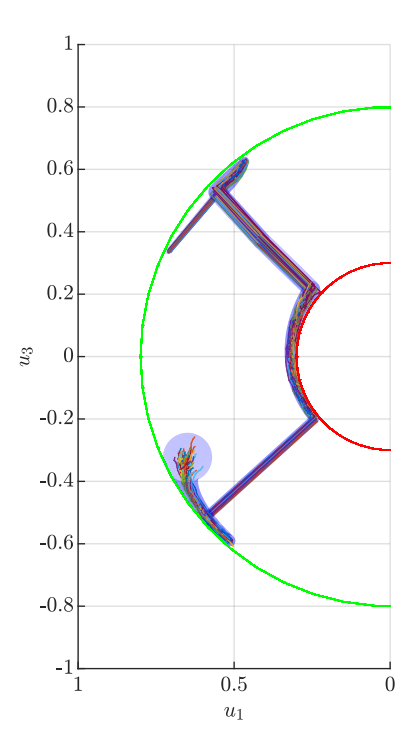


Figure 6: Select trajectories from a Monte Carlo simulation. The reference trajectory is depicted by a solid black line and the glide slope constraint is shown by a dashed line. The shaded region contains 99.9% of trajectories.



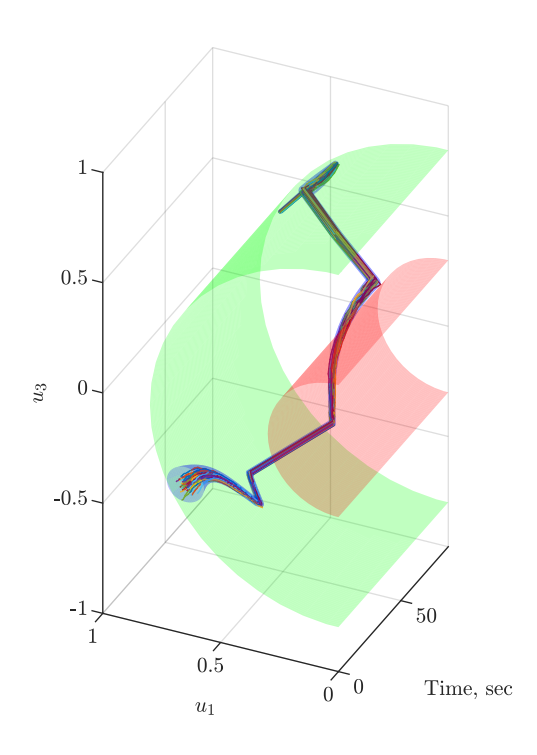
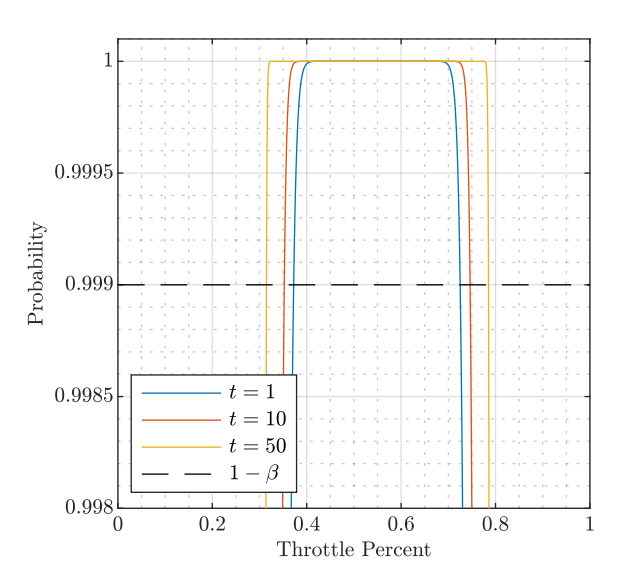


Figure 7: Normalized horizontal and vertical $(u_3 \text{ and } u_1)$ components of control, with maximum and minimum limits shown in green and red. Trials from a Monte Carlo are shown inside a tube containing $1-\beta$ probability.



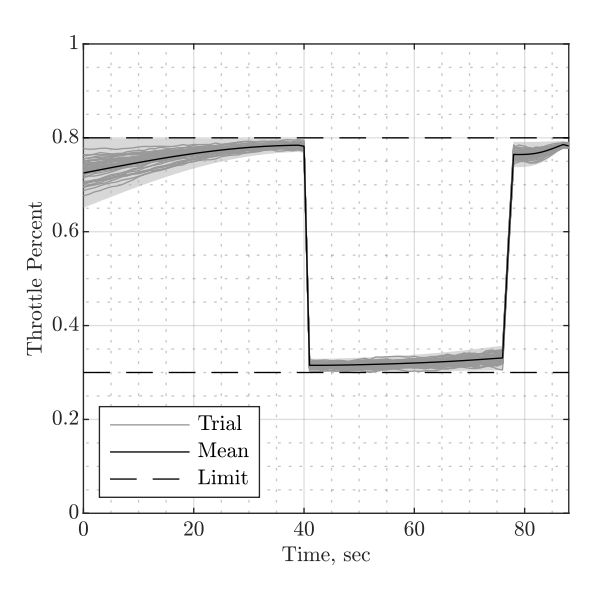


Figure 8: Left: probability that u is in Ω is plotted against the mean throttle percent at different times in the simulation. The values of ρ_1^{σ} and ρ_2^{σ} are determined by the left and right intersections of the probability curve with the dashed line for $1-\beta$, where $\beta=0.001$. Right: mean throttle percent and throttle histories from select Monte Carlo trials. The shaded region contains 99.9% of throttle histories.

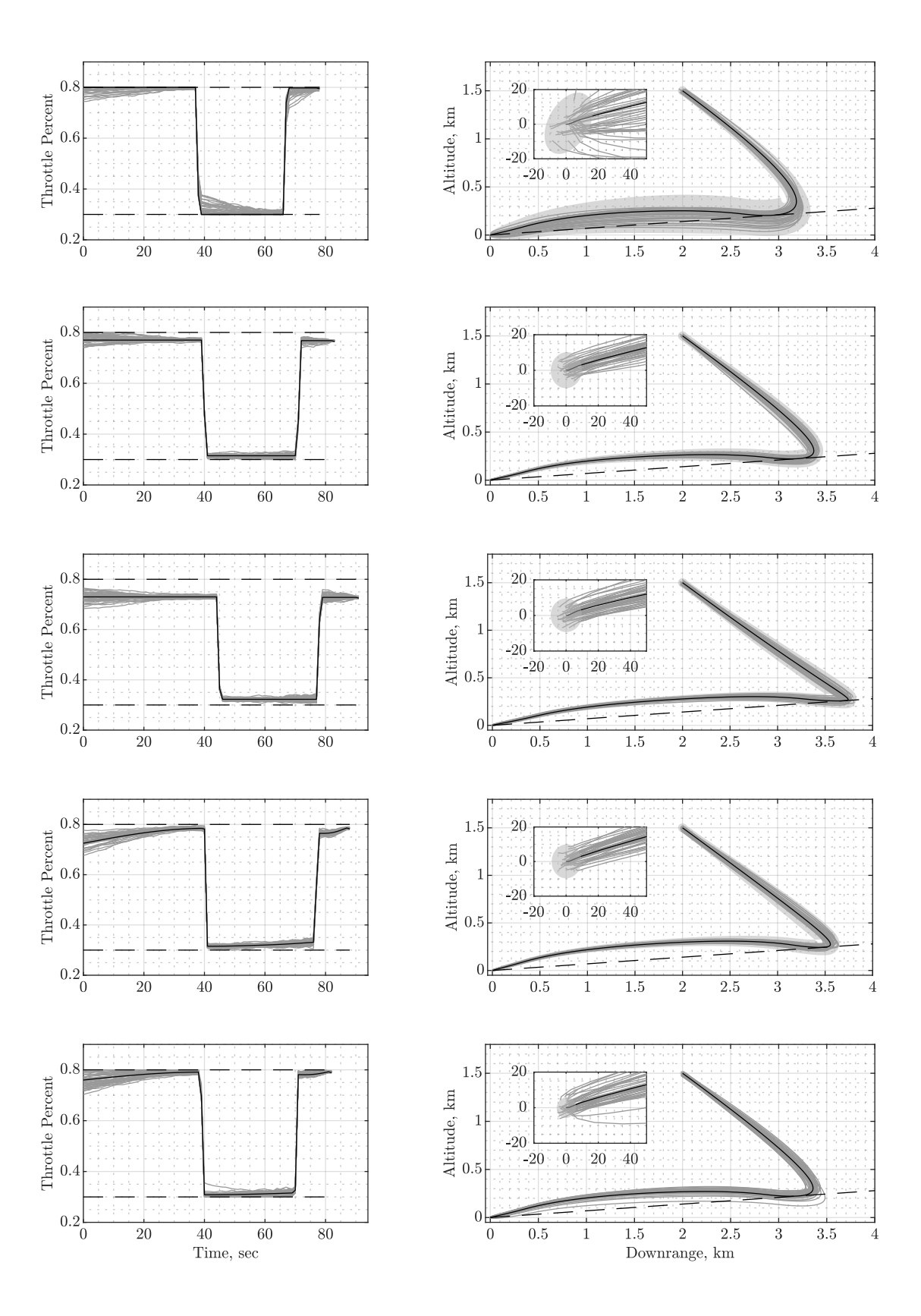


Figure 9: Comparison of proposed method to solutions obtained by varying ρ_i° as a constant bound. From top to bottom: bounds set to the absolute limit (i.e., no margin); constant bounds set, by trial and error, so that most trajectories reach the target despite control saturation; constant bounds set so that control will not saturate; bounds set by proposed method with $\beta=0.001$; and the proposed method with $\beta=0.5$. The shaded region on the trajectory plots contains 99.9% of trajectories, as calculated from 2,000 trial Monte Carlo trials, and the inset plots have units of meters.

powered descent dynamics into a deterministic mean and a stochastic perturbation. It was then shown that a probabilistic constraint on the control magnitude introduced in the trajectory design problem a dependence on the closed-loop system behavior, and this dependence caused the two problems to be coupled. For this reason, the covariance steering formulation was extended to the use of mass feedback so that the controller design is not mass dependent, and therefore the resulting CS-PDG guidance algorithm does not require any iteration and is suitable for onboard use. The proposed approach was then applied to an MSL powered divert scenario in a numerical simulation.

An interesting consequence of constraining the control bounds in probability was shown in Section VI. The baseline case with a small throttle margin resulted in saturated controls that did not satisfy this constraint, but in spite of this, the final state covariance target was nearly met. Since the control was often saturated in this case, the fuel cost was lower than the proposed method that constrained the control in probability. On the other hand, the proposed method fits into the existing theory on the control of state covariances, which allows us to precisely target final state covariances. In light of this observation, we are interested in studying the control of state covariances with bounded controls in a future work.

Acknowledgments

We thank Soumyo Dutta of the NASA Langley Research Center for valuable comments and discussions. This work was supported by a NASA Space Technology Research Fellowship.

References

- ¹B. Açıkmeşe and S. R. Ploen, "Convex programming approach to powered descent guidance for Mars landing," *Journal of Guidance, Control, and Dynamics*, vol. 30, pp. 1353–1366, September-Octover 2007.
- ²B. Açikmeşe, J. M. Carson III, and L. Blackmore, "Lossless convexification of nonconvex control bound and pointing constraints of the soft landing optimal control problem," *IEEE Transactions on Control Systems Technology*, vol. 21, no. 6, 2013.
- ³D. Dueri, S. V. Raković, and B. Açıkmeşe, "Consistently improving approximations for constrained controllability and reachability," in *Control Conference (ECC)*, 2016 European, pp. 1623–1629, IEEE, 2016.
- ⁴G. Singh, A. M. SanMartin, and E. C. Wong, "Guidance and control design for powered descent and landing on Mars," in 2007 IEEE Aerospace Conference, pp. 1–8, March 2007.
- ⁵E. C. Wong, G. Singh, and J. P. Masciarelli, "Guidance and control design for hazard avoidance and safe landing on Mars," *Journal of Spacecraft and Rockets*, vol. 43, no. 2, pp. 378–384, 2006.
- ⁶National Aeronautics and Space Administration, NASA Technology Roadmaps TA 9: Entry, Descent, and Landing Systems, July 2015.
- ⁷F. Alabau-Boussouira, R. Brockett, O. Glass, J. Le Rousseau, and E. Zuazua, Control of Partial Differential Equations, vol. 2048 of Lecture Notes in Mathematics. Cetraro, Italy: Springer, 2012.
- ⁸Y. Chen, T. T. Georgiou, and M. Pavon, "Optimal steering of a linear stochastic system to a final probability distribution, Part I," *IEEE Transactions on Automatic Control*, vol. 61, pp. 1158–1169, May 2016.
- ⁹Y. Chen, T. T. Georgiou, and M. Pavon, "Optimal steering of a linear stochastic system to a final probability distribution, Part II," *IEEE Transactions on Automatic Control*, vol. 61, pp. 1170–1180, May 2016.
- ¹⁰Y. Chen, T. T. Georgiou, and M. Pavon, "Optimal steering of a linear stochastic system to a final probability distribution, Part III," *IEEE Transactions on Automatic Control*, vol. 63, pp. 3112 – 3118, August 2016.
- ¹¹M. Goldshtein and P. Tsiotras, "Finite-horizon covariance control of linear time-varying systems," in *IEEE 56th Annual Conference on Decision and Control (CDC)*, (Melbourne, Australia), pp. 3606–3611, December 2017.
- ¹²R. Wheeden, R. Wheeden, and A. Zygmund, Measure and Integral: An Introduction to Real Analysis. Chapman & Hall/CRC Pure and Applied Mathematics, Taylor & Francis, 1977.
- ¹³U. Topcu, J. Casoliva, and K. D. Mease, "Minimum-fuel powered descent for Mars pinpoint landing," *Journal of Spacecraft and Rockets*, vol. 44, pp. 324–331, March-April 2007.
- ¹⁴J. Ridderhof and P. Tsiotras, "Uncertainty quantification and control during Mars powered descent and landing using covariance steering," in 2018 AIAA Guidance, Navigation, and Control Conference, no. AIAA 2018-0611, (Kissimmee, Flordia), 2018.
- ¹⁵G. Freiling, G. Jank, and H. Abou-Kandil, "Generalized Riccati difference and differential equations," *Linear Algebra and its Applications*, vol. 241, pp. 291–303, 1996.
- ¹⁶B. Açıkmeşe, J. M. Carson III, and D. S. Bayard, "A robust model predictive control algorithm for incrementally conic uncertain/nonlinear systems," *International Journal of Robust and Nonlinear Control*, vol. 21, no. 5, pp. 563–590, 2011.
- ¹⁷M. Athans and P. L. Falb, Optimal Control: An Introduction to the Theory and Its Applications. Lincoln Laboratory Publications, McGraw-Hill, 1966.